

000 001 002 003 004 005 006 007 008 009 010 011 012 013 014 015 016 017 018 019 020 021 022 023 024 025 026 027 028 029 030 031 032 033 034 035 036 037 038 039 040 041 042 043 044 045 046 047 048 049 050 051 052 053 LONGHORIZONUI: A UNIFIED FRAMEWORK FOR ROBUST LONG-HORIZON TASK AUTOMATION OF GUI AGENT

Anonymous authors

Paper under double-blind review

ABSTRACT

While multimodal large language models (MLLMs) have shown promise in short-horizon GUI agents, their performance degrades significantly on long-horizon tasks involving complex, dynamic interfaces. To address this, we present LongHorizonUI, a framework designed to enhance the reliability and robustness of MLLM-based agents in extended interactive environments. Moreover, we establish a new long-horizon benchmark, named LongGUIDBench, encompassing complex general applications and various gaming scenarios. Long-horizon tasks in this benchmark are defined as those requiring more than 15 steps, enabling thorough evaluation of long-horizon reasoning capabilities. Building upon this benchmark, we develop a Multimodal Enhanced Perceiver that integrates element detection and text recognition models, assigning unique indices to interface elements, thereby reinforcing state representation. Furthermore, we introduce a Deep-Reflection Decider, which employs a structured multi-level feedback-validation mechanism to support iterative reasoning and guarantee precise action execution along predictable trajectories. Building on the Deciders outputs, a Compensatory Action Executor continuously monitors execution progress; when degradation is detected, it applies targeted compensation operations or triggers a rollback procedure, thereby maintaining robustness throughout long-horizon tasks. Experiments show that LongHorizonUI substantially improves long-horizon performance on LongGUIDBench, while remaining competitive on diverse public benchmarks. The code and models will be publicly available.

1 INTRODUCTION

Graphical user interface (GUI) agents (Hong et al., 2024; Wang et al., 2025; Huang et al., 2025; Ye et al., 2025; Tan et al., 2024) are increasingly utilized in dynamic interactive environments to automate diverse workflows. The advancement of multimodal large language models (MLLMs) (Liu et al., 2023; Li et al., 2023; Lin et al., 2024; Zhang et al., 2024) has notably bolstered the capabilities of GUI agents in tackling more intricate scenarios, enabling them not only to handle simple, short-term tasks (Hong et al., 2024; Sun et al., 2025a) but also to engage in complex, long-horizon interactions within gaming environments and enterprise applications.

Recent work (Sun et al., 2025b; Fan et al., 2025) has investigated online reinforcement learning to improve adaptability by generating training data through environmental interactions. However, the trial-and-error learning paradigm expands the action space and amplifies cumulative errors over long horizons. Moreover, most of the existing benchmarks (Li et al., 2024a; Lu et al., 2024a; Chai et al., 2025; Rawles et al., 2023) are designed for short-term tasks typically fewer than 15 steps, as shown in Figure 2a, and thus fail to support long-horizon evaluations. Consequently, developing reliable GUI agents in long-horizon tasks remains a significant challenge.

Key Observations. To investigate the challenge of current methods in the long-horizon task scenarios, we conduct experiments by evaluating state-of-the-art methods (Liu et al., 2025; Qin et al., 2025; Zhang et al., 2025) on the AndroidControl benchmark (Li et al., 2024a) across sequences of varying lengths, as shown in Figure 2b. Specifically, for sequences with ≤ 5 steps, average success rates exceed 90.0%. However, performance degrades sharply as sequence length increases. When

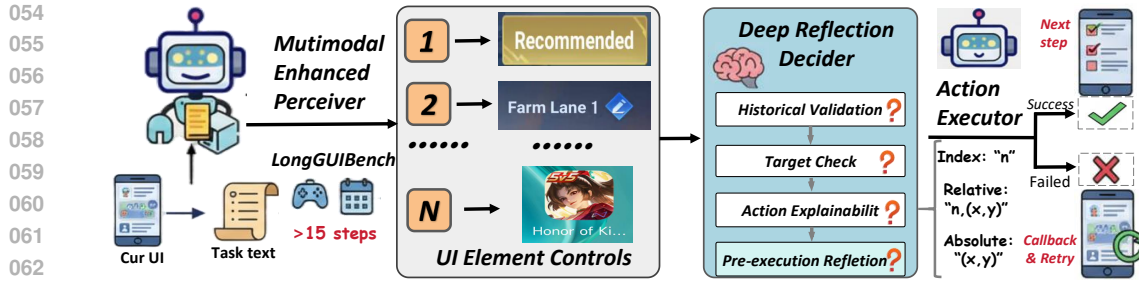


Figure 1: LongHorizonUI first builds an indexed element set (icons/text) via enhanced perception, next drives the MLLM with a structured prompt to validate history and derive multiple action candidates, and finally applies a three-stage executor (index, relative, absolute) with monitoring. This pipeline sustains reliable execution on sequences exceeding 15 steps.

sequences exceed 10 steps, the average success rate drops below 75%; for sequences longer than 15 steps, it falls to approximately 60%.

This non-linear performance degradation clearly indicates that current methods may fail to capture long-horizon state dependencies, allowing errors to accumulate exponentially as sequence length increases. Once the sequence length exceeds a certain threshold, the agent system collapses due to the inability to maintain cross-step contextual consistency. To address this issue, we need to answer the question: *how can we design GUI agents that maintain contextual coherence and decision-making proficiency over long-horizon action sequences?*

Our Solution. In this work, we propose LongHorizonUI, a framework for enhancing the robustness of MLLM-based GUI agents in complex and long-horizon tasks, as shown in Figure 1. Specifically, first, we propose a Multimodal Enhanced Perceiver (MEP) that integrates object detection and OCR outputs to capture rich contextual information, assigning indices to UI elements for temporally consistent state representation. Then, we design a Deep Reflection Decider (DRD) that performs structured, multi-level reasoning through formatted prompts, enforcing explicit validation of historical coherence, goal relevance, and action justification to ensure the decision fidelity. Finally, we incorporate a Compensatory Action Executor (CAE) that implements a multi-level fallback strategy by leveraging the element indices, relative layout priors, and absolute screen coordinates. Concurrently, a real-time progress monitor captures screen states and execution outcomes to construct a temporal state chain, enabling reliable rollback and recovery from execution errors.

Moreover, to comprehensively evaluate the performance in long-horizon scenarios, we introduce LongGUIBench, a new benchmark that consists of tasks requiring more than 15 steps across diverse gaming and application scenarios. It comprises 371 scenarios: 207 from 13 games and 147 task chains from 15 apps. Data were collected by professional testers, 6 human experts, via synchronized actionscreen recording, followed by cross-modal alignment and standardized parsing. Extensive experiments on both existing benchmarks and the proposed LongGUIBench demonstrate that LongHorizonUI outperforms existing methods by over 3% in task success rate, without sacrificing the generic performance.

To summarize, our contributions are as follows:

- We propose LongHorizonUI, a GUI agent designed for long-horizon reasoning, enhancing performance by an improved perceiver, a structured deep reflection decider, and a multi-level compensatory action executor.
- We introduce LongGUIBench, a new benchmark for long-horizon GUI interaction comprising diverse complex tasks from multiple application domains requiring more than 15 steps, with expert-annotated state trajectories and goal specifications.
- Extensive experiments on public benchmarks and LongGUIBench demonstrate that LongHorizonUI outperforms state-of-the-art methods in long-horizon tasks while maintaining competitive performance in standard settings, validating its efficacy and generalization capabilities.

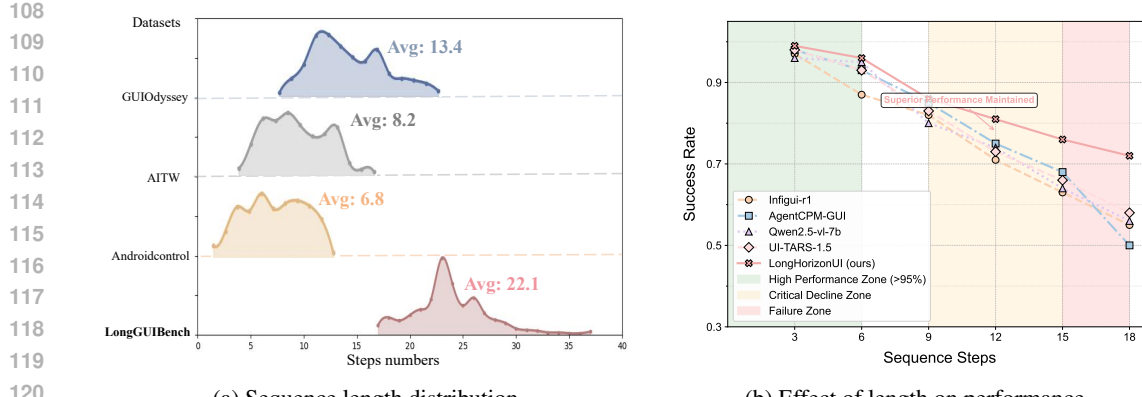


Figure 2: (a) Step-length distributions across GUI datasets. LongGUIBench shows markedly longer horizons (Avg: 22.1 steps) compared to GUIOdyssey (13.4), AITW (8.2), and AndroidControl (6.8), emphasizing evaluation beyond short episodes. (b) Success rate vs. sequence length on AndroidControl. All baselines degrade as horizons grow, with sharp drops beyond 10–15 steps; LongHorizonUI (ours) sustains higher SR and delays the critical decline, remaining competitive up to 18 steps.

2 OUR METHOD

In this section, as outlined in Figure 3, we introduce LongHorizonUI, a framework dedicated to long-horizon reasoning for GUI agents. Building upon the LongGUIBench benchmark spanning complex games and general application workflows, our approach integrates three core components: (i) a Multimodal Enhanced Perceiver integrating OCR and icon detection, (ii) a Deep Reflection Decider enabling action verification and adaptive planning, and (iii) a Compensatory Action Executor ensuring robust action execution. The following sections detail each element. The discussion of related work is in the Appendix C due to the page limit.

2.1 LONGGUIBENCH

In this section, we present LongGUIBench, a benchmark designed for evaluating long-horizon GUI tasks by simulating real-world, dynamic interactive scenarios. The dataset is constructed through synchronized collection of action sequences and screen snapshots, captured by professional testers as they execute predefined test cases across diverse applications and games. All tasks mandate at least 15 steps (mean steps: 22.1). Following cross-modal temporal alignment, the collected action commands and screenshots are input into MLLMs, leveraging structured prompts combined with screen perception algorithms, the MLLMs parse operation descriptions (e.g., “click the search bar”) and extract semantic control annotations, including button functionalities and bbox coordinates. This process generates a standardized intermediate representation with a key-value structure that includes the global descriptions (`task_name`) and decomposed sub-goal descriptions (`task_steps{action_ID, action_description, action_type, bbox, image_width/height}`). Finally, manual noise filtering yields a long-horizon dataset containing 371 scenarios.

Gaming Scenarios. Games typically involve complex interactive processes. To this end, we collaborate with professional testers to construct 207 high-complexity scenarios spanning 13 popular games, covering core mechanics such as equipment management and event participation. Each scenario is structured as a long-horizon task chain (19 to 37 steps, mean = 23.7 steps), captured in 4508 screen images to simulate real player decision flows. Each task includes two levels of instructions: High-Level instructions (HL) define macro goals, such as “purchase item XX in the game store,” while Low-Level instructions (LL) are broken down into atomic operation sequences, such as “click the store button,” and “click the purchase button.” Additionally, every operation step is annotated with fine-grained UI metadata, including control type (e.g., button, text box, drop-down menu), bbox coordinates, and state attributes.

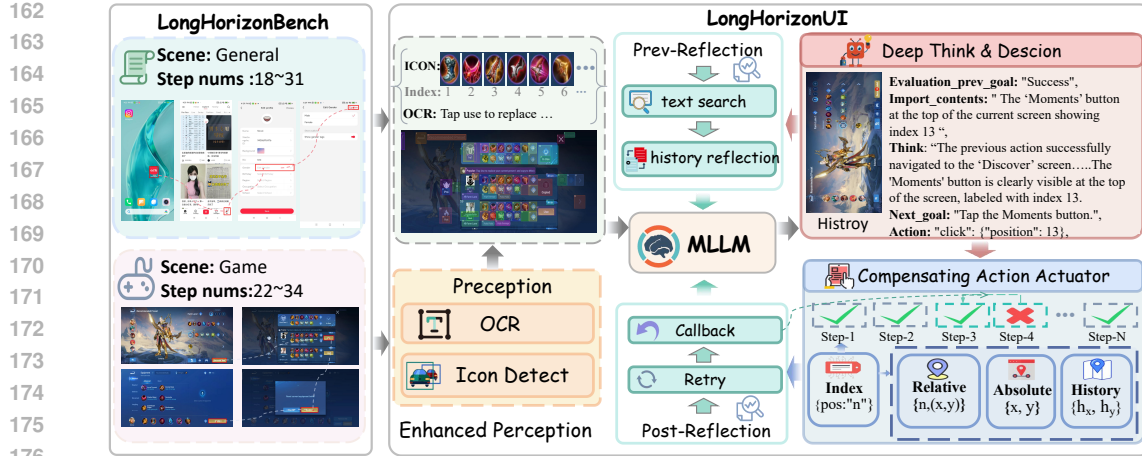


Figure 3: Illustration of LongHorizonUI framework. The LongGUIBench is introduced to define complex long-horizon interaction scenarios. An enhanced perceiver (OCR + Icon detection) extracts enriched UI element features, while a deep reasoning engine performs three-tier closed-loop validation of action feasibility. The compensation actuator employs multi-stage strategies (index/relative/absolute/historical coordinates) for robust execution.

General Scenarios. To assess generalization capability, we constructed 147 end-to-end task chains across 15 popular apps, covering complete user workflows from trigger to feedback. Each task requires 15-27 actions (mean = 19.5) and incorporates both abstraction levels: High-level instructions define global goals (e.g., 'Schedule a 1.5-hour meeting starting at 10 am on June 29th'). Low-level instructions specify atomic operations (e.g., Launch Tencent Meeting; Click 'Schedule'; Select 'Standard Meeting'; Set duration). All steps are annotated with granular UI semantics, emphasizing complex interface behaviours (e.g., multi-level dropdown navigation, real-time input validation) to validate long-horizon GUI agents in challenging workflows.

2.2 MULTIMODAL ENHANCED PERCEIVER

Accurately identifying and disambiguating interactive elements in context is key to enabling task automation in complex GUIs. To this end, we propose the Multimodal Enhanced Perceiver (MEP), which unifies icon detection, OCR recognition, and heuristic repair into an ID-centred abstraction layer, extracting actionable signals from evolving GUIs, inspired by prior work (Lu et al., 2024c).

Specifically, given a GUI screenshot S , MEP extracts visual elements through parallel perception modules: (i) An enhanced detector identifies interactive controls, producing $E_{ui} = (id_i, b_i, c_i)_{i=1}^N$, with id_i a unique spatial tag, b_i its bounding box, and c_i the confidence from the detector head (**sigmoid class probability**). IDs serve as stable anchors, robust to small layout variations. MEP also **highlights previously clicked elements**. (ii) A conventional OCR module extracts $E_{text} = (t_j, b_j)_{j=1}^M$, with t_j the detected text and b_j the bounding box. To disambiguate composite controls such as icon + text, each $e_i \in E_{ui}$ is linked with its most relevant text via a semantic binding function:

$$\hat{e}_i = \Phi(e_i, E_{text}) = \begin{cases} (id_i, b_i \cup b_{j^*}, t_{j^*}, c_i), & \text{if } \text{IoU}(b_i, b_{j^*}) \geq \tau, \\ (id_i, b_i, \emptyset, c_i), & \text{otherwise,} \end{cases} \quad (1)$$

where $j^* = \arg \max_j \text{IoU}(b_i, b_j)$ denotes the text box with maximum overlap, and binding is applied only when $\text{IoU}(b_i, b_{j^*}) \geq \tau$ (Appendix 3).

To mitigate missed detections of critical elements, such as close buttons on pop-ups, we employ a fallback template matcher that is activated when no elements are detected in designated high-priority areas A_{priority} (**small normalized bands around pop-up corners and bottom bars where missing a control can stall a trajectory**). Upon activation, the module invokes a repair function \mathcal{R} over A_{priority} , leveraging a template library \mathcal{T} of canonical close/cancel, confirm/next, and back/home icons; **high-similarity matches are inserted as new elements only in these regions** to match and restore omitted key elements.

216 2.3 DEEP REFLECTION DECIDER
217

218 Current agent decision mechanisms (Niu et al., 2024; Kil et al., 2024) based on self-supervised
219 training paradigms exhibit limited long-horizon generalization due to constrained dataset diversity,
220 while MLLMs-based mechanisms (Wang et al., 2024), despite superior sequence modeling capa-
221 bilities, suffer from cascading error propagation under dynamic interface shifts, compromising re-
222 liability in long-horizon task execution. To address this, we propose the Deep Reflection Decider,
223 as illustrated in Figure 4, which implements a structured multi-level feedback mechanism to es-
224 tablish triple closed-loop reasoning. This strategy validates goal rationality pre-execution and confirms
225 environmental-state consistency post-execution, ensuring action precision and prediction credibility.

226 Specifically, a strictly defined JSON
227 Schema (fields: historical_status,
228 import_contents, think, Execute_goal,
229 action, further details are provided in Ap-
230 pendix 1.) enforces structured three-tier reasoning,
231 where the first three fields implement reflection
232 and the last two fields implement decision:

233 (1) *Historical Validation*: the historical
234 status validates UI state transitions (e.g., button
235 activation, text input) via OCR/icon detection,
236 establishing spatiotemporal verification loops.
237 Failure flags trigger root-cause analysis upon
238 detecting error dialogues or unresponsive elements.

239 (2) *Target Check*: the import_contents field
240 extracts screen-critical information, validating the
241 MLLM’s environmental comprehension via OCR/i-
242 con detection. Task-goal consistency assessments
243 retain high-relevance text while filtering noise.

244 (3) *Action Explainability*: the think field requires the MLLM to sequentially analyze current UI
245 states, failure causes (if any), and action localization rationale (e.g., “Button #12 has the highest
246 interaction confidence”), with outputs culminating in executable goals (Execute_goal) that are
247 translated into atomic actions (action).

248 **Pre-execution Reflection.** Before execution, each candidate action is screened for on-screen
249 grounding and task entailment. We accept a for execution only if
250

$$\phi(s_t, a | \mathcal{G}_t, \mathcal{T}) = \mathbf{1}[g_{tg}(a) \in \mathcal{G}_t] \wedge \mathbf{1}[K(d_{action}) \subseteq K(\mathcal{T})] = 1. \quad (2)$$

251 Here, \mathcal{G}_t denotes the UI elements at state s_t from the perceiver, \mathcal{T} the global task description, and
252 a a candidate action with (Execute_goal, action) and description d_{action} . $g_{tg}(a)$ is the target
253 element of a , and $K(\cdot)$ a keyword extractor enforces that the action semantics are consistent with the
254 task. In practice, if either the target element is absent from the current screen or the action semantics
255 are not entailed by the task description, the action is rejected and a brief revision step is triggered
256 using available OCR/icon evidence; otherwise, the action proceeds.

259 2.4 COMPENSATING ACTION EXECUTOR
260

261 Current MLLM-driven agents face actioninstruction uncertainty: free-format outputs lack a direct
262 mapping to executable screen coordinates, while dynamic UIs require real-time correction. To bridge
263 this semanticphysical gap, we introduce the **Compensating Action Executor (CAE)**, which adopt
264 a robust action pipeline with multi-stage compensation and progress-triggered backtracking (see
265 Algorithm 1).

266 **Compensating Action Execution.** We first parse element indices (e.g., position:13) and se-
267 mantic descriptions (e.g., Top Moments button) from the Deciders output, then resolve the target
268 elements bounding box from the live layout, denoted $B = (x_{min}, y_{min}, x_{max}, y_{max})$. Normal-
269 ized coordinates (x_{norm}, y_{norm}) are mapped to physical pixels using a **device-aware scaling matrix**

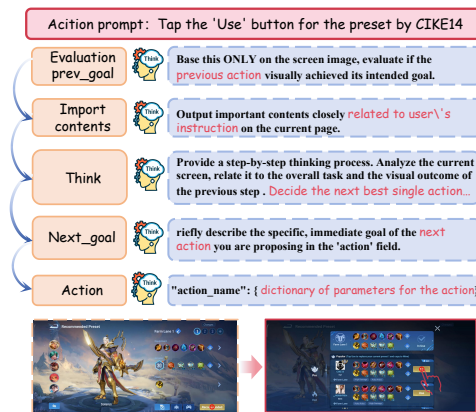


Figure 4: Deep reflection and decision-making processes designed to validate prior actions and predict subsequent steps.

270 **Algorithm 1** Compensating Action Executor (single step)

271

272 **Require:** Current state s_t ; candidates \mathcal{A} from DEEP REFLECTION DECIDER encoded as
 index(position: "i"), relative(action: "n, (x, y)"),
 absolute(point: "(x, y) + \epsilon"); last committed snapshot (s_{t-1}, p_{t-1})

273

274 **Ensure:** Executed (a^*, enc^*, p^*) with $\delta \in \{\text{SUCCESS, FAIL}\}$ (rollback on fail)

275 1: $\Pi \leftarrow [\text{index(position: "i")}, \text{relative(action: "n, (x, y)")},$
 276 $\text{absolute(point: "(x, y) + \epsilon")}]$ \triangleright priority: index \rightarrow relative \rightarrow absolute

277 2: **for each** $\text{enc} \in \Pi$ **do**

278 3: **if** $\exists a \in \mathcal{A}$ s.t. $\text{Encode}(a) = \text{enc}$ **then**

279 4: $p \leftarrow \text{RESOLVEPOINT}(a, \text{enc}, s_t)$ \triangleright centroid / element-local map / screen map + jitter

280 5: $\text{EXECUTECLICK}(p)$

281 6: $(s_{t+1}, \delta) \leftarrow \text{VERIFYMLLM}(s_t, a, p)$

282 7: **if** $\delta = \text{SUCCESS}$ **then**

283 8: **return** $(a, \text{enc}, p, \text{SUCCESS})$ \triangleright caller updates snapshot to (s_{t+1}, p)

284 9: **else**

285 10: **continue** \triangleright degrade to next encoding

286 11: **end if**

287 12: **end if**

288 13: **end for**

289 14: $\text{RECORDFAILURE}(s_t, \mathcal{A}); \text{ROLLBACK}(s_{t-1}, p_{t-1})$

15: **return** $(\perp, \perp, \perp, \text{FAIL})$

$S = \text{diag}(W_{\text{screen}}, H_{\text{screen}})$, with $p = S \cdot (x_{\text{norm}}, y_{\text{norm}})^\top$, so that the same normalized command is mapped consistently to device-specific click locations across different resolutions.

To enhance operational robustness, we employ a three-stage degradation policy consistent with our encodings `index(position:"i")`, `relative(action:"n,(x,y)")`, and `absolute(point:"(x,y) + ε")`:

- (1) *Index (centroid)*. Prioritize index-based execution at the element centroid p_0 of B ; i.e., the midpoints of the intervals $[x_{\min}, x_{\max}]$ and $[y_{\min}, y_{\max}]$.
- (2) *Relative (in-box)*. If the attempt fails ($\delta = 0$), draw a click p_{rel} uniformly inside B : sample $\lambda_w, \lambda_h \sim \mathcal{U}[0, 1]$ and place the point using the box width $w = x_{\max} - x_{\min}$ and height $h = y_{\max} - y_{\min}$.
- (3) *Absolute (screen) with jitter*. Upon repeated failure, use absolute screen coordinates mapped from (x, y) and add a bounded perturbation ϵ (e.g., $\|\epsilon\|_\infty \leq 5$ px) to escape edge/occlusion cases; the base point defaults to the normalized target or p_0 when unspecified.

Post-execution Reflection. For each action instruction a at state s_t , we execute its candidates in the stated priority order. After each attempt, the DEEP REFLECTION DECIDER performs state verification:

$$v_t = \text{Verify}_{\text{MLLM}}(s_t, a, p_t, I_{t+1}) \in \{0, 1\}. \quad (3)$$

where p_t is the click point computed from the current attempt and the resolved box B , and I_{t+1} is the post-action screenshot. If $v_t = 1$, we commit the step and update the snapshot to (s_{t+1}, p_t) . Otherwise, we degrade to the next candidate. When all candidates for a are rejected, we allow a few local re-planning calls to DRD at the same state; if these still fail, we invoke $\text{Rollback}(s_{t-1}, p_{t-1})$ to restore the last committed snapshot and continue execution. (see Appendix 5 for details and statistics).

3 EXPERIMENTS

3.1 IMPLEMENTATION DETAILS

To ensure fair evaluation across benchmarks, we select base models aligned with their architectures and configure consistent experimental settings. For LongHorizonBench, we adopt a representative MLLMs (Comanici et al., 2025) as the backbone to ensure stable reasoning in long-horizon tasks.

324 Table 1: Performance Comparison of Models on LongGUIBench Long-Horizon Tasks
325

326 327 328 329 330 331 332 333 334 335 336 337 338 339 340 341 342 343 344 345 346 347 348 349 350 351 352 353 354 355 356 357 358 359 360 361 362 363 364 365 366 367 368 369 370 371 372 373 374 375 376 377 Model Name	326 327 328 329 330 331 332 333 334 335 336 337 338 339 340 341 342 343 344 345 346 347 348 349 350 351 352 353 354 355 356 357 358 359 360 361 362 363 364 365 366 367 368 369 370 371 372 373 374 375 376 377 General-Low		326 327 328 329 330 331 332 333 334 335 336 337 338 339 340 341 342 343 344 345 346 347 348 349 350 351 352 353 354 355 356 357 358 359 360 361 362 363 364 365 366 367 368 369 370 371 372 373 374 375 376 377 General-High		326 327 328 329 330 331 332 333 334 335 336 337 338 339 340 341 342 343 344 345 346 347 348 349 350 351 352 353 354 355 356 357 358 359 360 361 362 363 364 365 366 367 368 369 370 371 372 373 374 375 376 377 Game_Low		326 327 328 329 330 331 332 333 334 335 336 337 338 339 340 341 342 343 344 345 346 347 348 349 350 351 352 353 354 355 356 357 358 359 360 361 362 363 364 365 366 367 368 369 370 371 372 373 374 375 376 377 Game_High		326 327 328 329 330 331 332 333 334 335 336 337 338 339 340 341 342 343 344 345 346 347 348 349 350 351 352 353 354 355 356 357 358 359 360 361 362 363 364 365 366 367 368 369 370 371 372 373 374 375 376 377 Avg
326 327 328 329 330 331 332 333 334 335 336 337 338 339 340 341 342 343 344 345 346 347 348 349 350 351 352 353 354 355 356 357 358 359 360 361 362 363 364 365 366 367 368 369 370 371 372 373 374 375 376 377 TM	326 327 328 329 330 331 332 333 334 335 336 337 338 339 340 341 342 343 344 345 346 347 348 349 350 351 352 353 354 355 356 357 358 359 360 361 362 363 364 365 366 367 368 369 370 371 372 373 374 375 376 377 SR	326 327 328 329 330 331 332 333 334 335 336 337 338 339 340 341 342 343 344 345 346 347 348 349 350 351 352 353 354 355 356 357 358 359 360 361 362 363 364 365 366 367 368 369 370 371 372 373 374 375 376 377 Avg							
<i>Base Models</i>									
GPT-4o (OpenAI et al., 2024)	87.5	20.8	75.0	4.2	91.6	23.9	85.9	3.7	49.1
Gemini2.5 (Comanici et al., 2025)	96.7	73.3	77.2	25.7	95.1	57.7	84.3	25.7	67.3
Qwen2.5-VL-7b (Bai et al., 2025)	92.3	82.7	73.1	29.3	92.4	72.8	68.9	27.4	67.4
<i>GUI Models</i>									
OmniParser (Lu et al., 2024b)	90.0	83.0	79.3	35.6	91.8	61.0	70.4	20.1	66.4
AgentCPM-GUI (Zhang et al., 2025)	92.1	81.2	82.4	37.1	89.7	66.5	74.1	25.8	68.6
InfiGUI-R1 (Liu et al., 2025)	93.2	79.7	56.7	23.8	92.9	67.2	53.9	19.4	61.8
UI-TARS-1.5 (Qin et al., 2025)	93.6	79.2	75.4	21.8	88.2	69.5	77.8	18.9	65.8
LongHorizonUI	93.5	85.3	78.0	52.3	93.8	83.9	79.7	52.1	77.3

339 Table 2: Grounding Performance Comparison on the ScreenSpot Benchmark.
340

341 342 343 344 345 346 347 348 349 350 351 352 353 354 355 356 357 358 359 360 361 362 363 364 365 366 367 368 369 370 371 372 373 374 375 376 377 Model Name	341 342 343 344 345 346 347 348 349 350 351 352 353 354 355 356 357 358 359 360 361 362 363 364 365 366 367 368 369 370 371 372 373 374 375 376 377 Mobile		341 342 343 344 345 346 347 348 349 350 351 352 353 354 355 356 357 358 359 360 361 362 363 364 365 366 367 368 369 370 371 372 373 374 375 376 377 Desktop		341 342 343 344 345 346 347 348 349 350 351 352 353 354 355 356 357 358 359 360 361 362 363 364 365 366 367 368 369 370 371 372 373 374 375 376 377 Web		341 342 343 344 345 346 347 348 349 350 351 352 353 354 355 356 357 358 359 360 361 362 363 364 365 366 367 368 369 370 371 372 373 374 375 376 377 Avg	
341 342 343 344 345 346 347 348 349 350 351 352 353 354 355 356 357 358 359 360 361 362 363 364 365 366 367 368 369 370 371 372 373 374 375 376 377 TM	341 342 343 344 345 346 347 348 349 350 351 352 353 354 355 356 357 358 359 360 361 362 363 364 365 366 367 368 369 370 371 372 373 374 375 376 377 SR	341 342 343 344 345 346 347 348 349 350 351 352 353 354 355 356 357 358 359 360 361 362 363 364 365 366 367 368 369 370 371 372 373 374 375 376 377 Avg	341 342 343 344 345 346 347 348 349 350 351 352 353 354 355 356 357 358 359 360 361 362 363 364 365 366 367 368 369 370 371 372 373 374 375 376 377 Text	341 342 343 344 345 346 347 348 349 350 351 352 353 354 355 356 357 358 359 360 361 362 363 364 365 366 367 368 369 370 371 372 373 374 375 376 377 Icon	341 342 343 344 345 346 347 348 349 350 351 352 353 354 355 356 357 358 359 360 361 362 363 364 365 366 367 368 369 370 371 372 373 374 375 376 377 Text	341 342 343 344 345 346 347 348 349 350 351 352 353 354 355 356 357 358 359 360 361 362 363 364 365 366 367 368 369 370 371 372 373 374 375 376 377 Icon		
<i>Base Models</i>								
GPT-4o (OpenAI et al., 2024)	30.5	23.2	20.6	19.4	11.1	7.8	18.8	
Gemini2.0 (Comanici et al., 2025)	—	—	—	—	—	—	84.0	
Qwen2.5-VL-7b (Bai et al., 2025)	—	—	—	—	—	—	84.7	
<i>GUI Models</i>								
CogAgent (Hong et al., 2024)	67.0	24.0	74.2	20.0	70.4	28.6	47.4	
SeeClick (Cheng et al., 2024)	78.0	52.0	72.5	30.0	55.7	32.5	53.4	
ShowUI (Lin et al., 2025)	92.3	75.5	76.3	61.1	81.7	63.6	75.1	</td

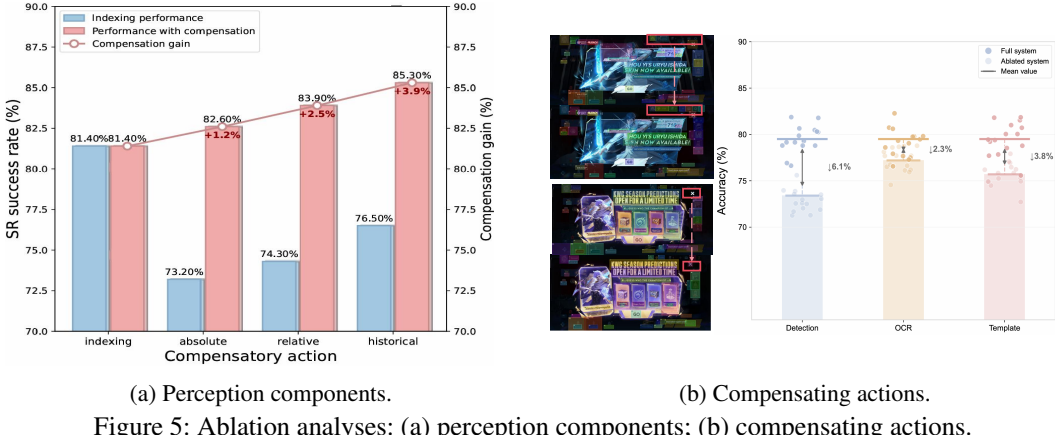


Figure 5: Ablation analyses: (a) perception components; (b) compensating actions.

LongHorizonUI reaches a low-level instruction SR of 83.9% and a high-level instruction SR of 52.1%, which maintains a clear lead across all compared methods. These results validate the proposed LongHorizonUI’s significant advantage in modeling long-horizon dependencies.

Grounding Capability. Table 2 compares our LongHorizonUI framework with mainstream methods on the ScreenSpot dataset, including base models and SOTA GUI agents. LongHorizonUI demonstrates consistent superiority across device subsets (mobile, desktop, web), achieving 90.4% average task success rate, surpassing all open-source models and outperforming the previous SOTA GUI framework (UI-TARS) by 2.9%. These results validate LongHorizonUI’s robust grounding capability across diverse devices and scenarios.

Navigation Capability. To rigorously evaluate the navigation capabilities of our method, we benchmarked LongHorizonUI against state-of-the-art approaches on AndroidControl (Li et al., 2024a) and GUI-Odyssey (Lu et al., 2024a). As shown in Table 3, LongHorizonUI achieves significant improvements in SR over both zero-shot models and GUI-specialized baselines. Compared to Qwen2.5-VL-7B, our method elevates SR by 6.4% on AndroidControl-High and 6.1% on GUI-Odyssey. Moreover, LongHorizonUI attains an average SR gain of 2.3% over the strong GUI-R1-7B baseline. These results demonstrate that LongHorizonUI not only significantly enhances planning robustness for long-horizon tasks but also retains fundamental interaction capabilities for short sequences.

Table 3: Performance comparison on AndroidControl and GUI-Odyssey benchmarks

Model Type	Model Name	AndroidControl-Low		AndroidControl-High		GUI-Odyssey		Avg
		TM	SR	TM	SR	TM	SR	
Base Models	GPT-4o	74.3	28.4	63.1	21.2	37.5	5.4	38.3
	Qwen2.5-VL-3B	62.0	59.3	47.8	38.9	37.4	26.7	45.4
	Qwen2.5-VL-7B	83.4	62.5	68.7	47.1	55.6	34.4	58.6
GUI model	OS-Atlas-4B	64.6	40.6	49.0	22.8	49.6	20.3	41.1
	Os-Atlas-7B	73.0	50.9	57.4	29.8	60.4	27.0	49.8
	GUI-R1-3B	83.7	64.4	58.0	46.6	54.8	41.3	58.1
	GUI-R1-7B	85.2	66.5	71.6	51.7	65.5	38.8	63.2
Ours	LongHorizonUI	87.5	68.9	73.4	54.2	68.3	40.5	65.5

3.4 ABLATION STUDY

Effectiveness of Perception Components. Figure 5a reports an ablation study that isolates each perception module. Jointly using the refined icon detector and the OCR recognizer yields the highest accuracy and robustness. Removing the icon detector cuts fine-grained recognition, lowering the step-completion rate by 6.1%. Disabling OCR causes the same 2.3% drop and leads to frequent errors on icon-text composite widgets. Turning off the adaptive grid prevents the detector from

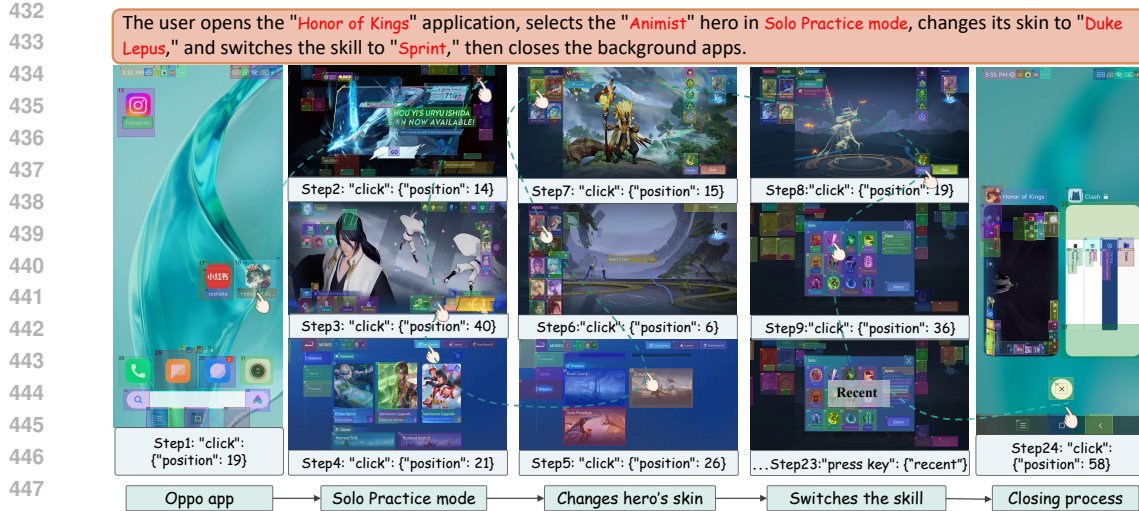


Figure 6: Case visualization of LongHorizonUI in a gaming scenario.

scaling to different screen resolutions, so microscopic elements on high-resolution displays are often missed. Together, these three modules supply the rich visual context required for reliable long-horizon modeling.

Effectiveness of Compensatory Actions. Figure 5b visually compares the different action modes, indexing instructions and step lengths, showing that indexing alone delivers an 81.4% task-completion rate, outperforming all other action modes. Adding compensatory actions on top of indexing gives further gains by 1.2% (relative coordinates), 2.5% (absolute coordinates), and 3.9% (historical coordinates). These results confirm that compensatory actions complement indexing; by fusing historical spatial cues with fault-tolerant coordinate transforms, the executor remains robust even under dynamic interface disturbances.

3.5 CASE VISUALIZATION

As illustrated in Figure 6, the LongHorizonUI agent executes a fully automated operation sequence in the Honor of Kings scenario. Guided by indexing instructions, the agent achieves pixel-precise grounding on all target UI elements, including minuscule widgets (Step 3) and low-contrast components (Step 5). Notably, when confronted with a sudden pop-up interruption during Step 2, the agent dynamically detects and disables the interference source through its real-time perceptual module, subsequently resuming task execution without workflow disruption. This end-to-end workflow spans multi-step operations from application launch, skill switching, to background process management, demonstrating LongHorizonUIs capability to maintain cross-step operational precision and dynamic disturbance robustness in complex task chains.

4 CONCLUSION

Summary. In this work, we present LongHorizonUI, an innovative framework for long-horizon GUI tasks, featuring a multimodal enhanced perceptron for precise capture of UI element states, a three-tier closed-loop reasoning engine for action verification/prediction, and an innovative multi-level compensator ensuring action execution validity. Demonstrating superior performance on Long-GUIBench (15-step tasks) and public benchmarks, it establishes a new paradigm for reliable long-horizon GUI tasks.

Limitations & Future Work. Despite achieving state-of-the-art performance without introducing notable overhead relative to prior agents, LongHorizonUI still inherits the latency of MLLM-dependent pipelines. Next, we will focus on model-level efficiency distillation, quantization, and context-aware prompt compression.

486 **ETHICS CHECKLIST**
487

488 **1. Code of Ethics Acknowledgement**
489

490 1.1. All authors have read and will adhere to the ICLR Code of Ethics; acknowledgement was made
491 during submission (yes/no) **yes**
492

493 1.2. This paper includes an Ethics Statement at the end of the main text, before references (if appli-
494 cable) (yes/no) **yes**
495

496 **2. Human Subjects and IRB/Consent**
497

498 2.1. Research involves human subjects or user studies (yes/no) **NA**
499

500 If yes, address the following:

501 2.2. IRB/ethics board approval (or equivalent) is obtained and documented (yes/NA) **NA**
502

503 2.3. Informed consent procedures are described; compensation and inclusion of minors are
504 disclosed (yes/NA) **NA**
505

506

507 **3. Data, Privacy, and Security**
508

509 3.1. All datasets used are cited with licenses and access conditions; non-public data are described
510 with justification (yes/partial/no) **yes**
511

512 3.2. Personally identifiable information (PII) was removed, anonymized, or processed under com-
513 pliant safeguards (yes/NA) **yes**
514

515 3.3. Data collection respects terms of service and legal/compliance requirements (e.g., copyright,
516 web scraping policies) (yes/partial/no) **yes**
517

518 3.4. Security-sensitive artifacts or vulnerabilities are responsibly handled (e.g., redactions, coordi-
519 nated disclosure) (yes/NA) **NA**
520

521 **4. Bias, Fairness, and Potential Harm**
522

523 4.1. Known risks of harmful or dual-use applications are discussed with mitigation strategies (yes/-
524 partial/no) **yes**
525

526 4.2. Bias/fairness concerns (subgroup performance, demographic or domain skews) are analyzed or
527 acknowledged (yes/partial/no) **partial**
528

529 4.3. Limitations, open risks, and appropriate use/disallowed use are stated (yes/no) **yes**
530

531 **5. Conflicts of Interest and Sponsorship**
532

533 5.1. All funding sources, compute donations, and in-kind support are disclosed (yes/no) **yes**
534

535 5.2. Potential conflicts of interest (employment, consulting, equity) are disclosed (yes/NA) **NA**
536

537 **6. Research Integrity**
538

539 6.1. All results are reported faithfully; negative findings or failure cases are included when relevant
(yes/partial/no) **yes**

540 6.2. Figures/tables are accurately labeled; data provenance and documentation are maintained (yes/-
 541 partial/no) **yes**
 542

543 *Note: The Ethics Statement is optional but recommended; it does not count toward the page limit and should
 544 not exceed one page.*
 545

546 **REPRODUCIBILITY CHECKLIST**

547 **7. Overall Documentation**

548 7.1. High-level method overview and/or pseudocode provided (yes/partial/no) **yes**
 549
 550 7.2. Clear separation of claims vs. evidence; notation and assumptions are stated (yes/partial/no)
 551 **yes**
 552
 553 7.3. Pointers to background/pedagogical resources for replication (yes/no) **yes**
 554
 555

556 **8. Code, Artifacts, and Environment**

557 8.1. Anonymous, downloadable code provided as supplementary material or link (yes/partial/no)
 558 **yes**
 559
 560 8.2. Exact commit/version, dependency list (e.g., environment.yml/requirements.txt),
 561 and OS details (yes/partial/no) **yes**
 562
 563 8.3. Hardware details (GPU/CPU models, RAM), framework/library versions, and runtime esti-
 564 mates (yes/partial/no) **yes**
 565
 566 8.4. Randomness handling documented (seeds, nondeterministic ops, determinism limits) (yes/par-
 567 tial/no/NA) **yes**
 568
 569

570 **9. Data and Preprocessing**

571 9.1. All datasets cited with URLs/licensing; custom splits or filtering rules documented (yes/par-
 572 tial/no) **yes**
 573
 574

575 **10. Training and Hyperparameters**

576 10.1. Search spaces and selection criteria reported; final hyperparameters listed per model (yes/par-
 577 tial/no) **yes**
 578
 579 10.2. Training schedules, batch sizes, losses, and early-stopping criteria documented (yes/partial/no)
 580 **yes**
 581
 582

583 **11. Evaluation and Reporting**

584 11.1. Metrics are formally defined and motivated; evaluation scripts included (yes/partial/no) **yes**
 585
 586 11.2. Number of runs, variance (e.g., std/CI), and significance tests reported where appropriate (yes/-
 587 partial/no) **partial**
 588
 589 11.3. Ablations/diagnostics provided to support claims and clarify failure modes (yes/partial/no) **yes**
 590
 591

592 **REFERENCES**

593 Jinze Bai, Shuai Bai, Yunfei Chu, and Zeyu Cui et al. Qwen technical report, 2023.

594 Shuai Bai, Keqin Chen, Xuejing Liu, Jialin Wang, Wenbin Ge, Sibo Song, Kai Dang, Peng Wang,
 595 Shijie Wang, Jun Tang, Humen Zhong, Yuanzhi Zhu, Mingkun Yang, Zhaohai Li, Jianqiang Wan,
 596 Pengfei Wang, Wei Ding, Zheren Fu, Yiheng Xu, Jiabo Ye, Xi Zhang, Tianbao Xie, Zesen Cheng,
 597 Hang Zhang, Zhibo Yang, Haiyang Xu, and Junyang Lin. Qwen2.5-vl technical report. *arXiv*
 598 preprint *arXiv:2502.13923*, 2025.

599 Yuxiang Chai, Siyuan Huang, Yazhe Niu, Han Xiao, Liang Liu, Dingyu Zhang, Shuai Ren, and
 600 Hongsheng Li. Amex: Android multi-annotation expo dataset for mobile gui agents, 2025.
 601

602 Kanzhi Cheng, Qiushi Sun, Yougang Chu, Fangzhi Xu, Yantao Li, Jianbing Zhang, and Zhiyong
 603 Wu. Seeclick: Harnessing gui grounding for advanced visual gui agents, 2024.
 604

605 Gheorghe Comanici, Eric Bieber, Mike Schaeckermann, Ice Pasupat, Noveen Sachdeva, Inderjit
 606 Dhillon, Marcel Blstein, Ori Ram, Dan Zhang, Evan Rosen, et al. Gemini 2.5: Pushing the
 607 frontier with advanced reasoning, multimodality, long context, and next generation agentic capa-
 608 bilities. *arXiv preprint arXiv:2507.06261*, 2025.

609 Alexey Dosovitskiy, Lucas Beyer, Alexander Kolesnikov, Dirk Weissenborn, Xiaohua Zhai, Thomas
 610 Unterthiner, Mostafa Dehghani, Matthias Minderer, Georg Heigold, Sylvain Gelly, Jakob Uszko-
 611 reit, and Neil Houlsby. An image is worth 16x16 words: Transformers for image recognition at
 612 scale, 2021.

613 Yue Fan, Handong Zhao, Ruiyi Zhang, Yu Shen, Xin Eric Wang, and Gang Wu. Gui-bee: Align gui
 614 action grounding to novel environments via autonomous exploration, 2025.
 615

616 Hiroki Furuta, Kuang-Huei Lee, Ofir Nachum, Yutaka Matsuo, Aleksandra Faust, Shixiang Shane
 617 Gu, and Izzeddin Gur. Multimodal web navigation with instruction-finetuned foundation models,
 618 2024.

619 Wenyi Hong, Weihan Wang, Qingsong Lv, Jiazheng Xu, Wenmeng Yu, Junhui Ji, Yan Wang, Zihan
 620 Wang, Yuxiao Dong, Ming Ding, and Jie Tang. Cogagent: A visual language model for gui
 621 agents. In *Proceedings of the IEEE/CVF Conference on Computer Vision and Pattern Recognition*
 622 (CVPR), pp. 14281–14290, June 2024.

623 Zhiyuan Huang, Ziming Cheng, Junting Pan, Zhaohui Hou, and Mingjie Zhan. Spiritsight agent: Ad-
 624 vanced gui agent with one look. In *Proceedings of the Computer Vision and Pattern Recognition*
 625 Conference (CVPR), pp. 29490–29500, June 2025.

626 Jihyung Kil, Chan Hee Song, Boyuan Zheng, Xiang Deng, Yu Su, and Wei-Lun Chao. Dual-view
 627 visual contextualization for web navigation. In *Proceedings of the IEEE/CVF Conference on*
 628 *Computer Vision and Pattern Recognition (CVPR)*, pp. 14445–14454, June 2024.

629 Geunwoo Kim, Pierre Baldi, and Stephen McAleer. Language models can solve computer tasks.
 630 In A. Oh, T. Naumann, A. Globerson, K. Saenko, M. Hardt, and S. Levine (eds.), *Advances in*
 631 *Neural Information Processing Systems*, volume 36, pp. 39648–39677, 2023.

632 Hanyu Lai, Xiao Liu, Iat Long Iong, Shuntian Yao, Yuxuan Chen, Pengbo Shen, Hao Yu, Hanchen
 633 Zhang, Xiaohan Zhang, Yuxiao Dong, and Jie Tang. Autowebglm: A large language model-based
 634 web navigating agent. In *Proceedings of the 30th ACM SIGKDD Conference on Knowledge*
 635 *Discovery and Data Mining*, pp. 52955306, 2024.

636 Sunjae Lee, Junyoung Choi, Jungjae Lee, Munim Hasan Wasi, Hojun Choi, Steven Y. Ko, Sangeun
 637 Oh, and Insik Shin. Explore, select, derive, and recall: Augmenting llm with human-like memory
 638 for mobile task automation, 2024.

639 Junnan Li, Dongxu Li, Silvio Savarese, and Steven Hoi. Blip-2: Bootstrapping language-image
 640 pre-training with frozen vision encoders and large language models. In *Proceedings of the Inter-*
 641 *national Conference on Machine Learning (ICML)*, pp. 19730–19742, 2023.

642 Wei Li, William Bishop, Alice Li, Chris Rawles, Folawiyo Campbell-Ajala, Divya Tyamagundlu,
 643 and Oriana Riva. On the effects of data scale on computer control agents. *arXiv preprint*
 644 *arXiv:2406.03679*, 2024a.

648 Yanda Li, Chi Zhang, Wanqi Yang, Bin Fu, Pei Cheng, Xin Chen, Ling Chen, and Yunchao Wei.
 649 Appagent v2: Advanced agent for flexible mobile interactions, 2024b.
 650

651 Bin Lin, Zhiyuan Ye, Shuyang Zhang, Jun He, and Dong Yu. Moe-llava: Mixture of experts for
 652 large vision-language models. In *Proceedings of the IEEE/CVF Conference on Computer Vision
 653 and Pattern Recognition (CVPR)*, pp. 13245–13255, June 2024.

654 Kevin Qinghong Lin, Linjie Li, Difei Gao, Zhengyuan Yang, Shiwei Wu, Zechen Bai, Stan Weixian
 655 Lei, Lijuan Wang, and Mike Zheng Shou. Showui: One vision-language-action model for gui
 656 visual agent. In *Proceedings of the Computer Vision and Pattern Recognition Conference (CVPR)*,
 657 pp. 19498–19508, June 2025.

658 Haotian Liu, Chunyuan Li, Yuheng Li, and Yong Jae Lee. Visual instruction tuning with large
 659 language models. In *Advances in Neural Information Processing Systems (NeurIPS)*, pp. 5189–
 660 5210, December 2023.

662 Yuhang Liu, Pengxiang Li, Congkai Xie, Xavier Hu, Xiaotian Han, Shengyu Zhang, Hongxia Yang,
 663 and Fei Wu. Infigui-rl: Advancing multimodal gui agents from reactive actors to deliberative
 664 reasoners, 2025.

666 Quanfeng Lu, Wenqi Shao, Zitao Liu, Fanqing Meng, Boxuan Li, Botong Chen, Siyuan Huang,
 667 Kaipeng Zhang, Yu Qiao, and Ping Luo. Gui odyssey: A comprehensive dataset for cross-app gui
 668 navigation on mobile devices, 2024a.

669 Yadong Lu, Jianwei Yang, Yelong Shen, and Ahmed Awadallah. Omniparser for pure vision based
 670 gui agent, 2024b.

671

672 Yadong Lu, Jianwei Yang, Yelong Shen, and Ahmed Awadallah. Omniparser for pure vision based
 673 GUI agent, 2024c.

674

675 Run Luo, Lu Wang, Wanwei He, and Xiaobo Xia. Gui-r1 : A generalist r1-style vision-language
 676 action model for gui agents, 2025.

677 Runliang Niu, Jindong Li, Shiqi Wang, Yali Fu, Xiyu Hu, Xueyuan Leng, He Kong, Yi Chang, and
 678 Qi Wang. Screenagent: A vision language model-driven computer control agent. In *Proceed-
 679 ings of the Thirty-Third International Joint Conference on Artificial Intelligence*, pp. 64336441.
 680 International Joint Conferences on Artificial Intelligence Organization, August 2024.

681 OpenAI, Josh Achiam, Steven Adler, and Sandhini Agarwal et al. Gpt-4 technical report, 2024.

682

683 Pranav Putta, Edmund Mills, Naman Garg, Sumeet Motwani, Chelsea Finn, Divyansh Garg, and
 684 Rafael Rafailov. Agent q: Advanced reasoning and learning for autonomous ai agents, 2024.

685

686 Yujia Qin, Yining Ye, Junjie Fang, Haoming Wang, and Shihao Liang et al. Ui-tars: Pioneering
 687 automated gui interaction with native agents, 2025.

688 Alec Radford, Jong Wook Kim, Chris Hallacy, Aditya Ramesh, Gabriel Goh, Sandhini Agarwal,
 689 Girish Sastry, Amanda Askell, Pamela Mishkin, Jack Clark, Gretchen Krueger, and Ilya Sutskever.
 690 Learning transferable visual models from natural language supervision, 2021.

691

692 Christopher Rawles, Alice Li, Daniel Rodriguez, Oriana Riva, and Timothy Lillicrap. An-
 693 droidinthewild: A large-scale dataset for android device control. In *Advances in Neural Infor-
 694 mation Processing Systems*, volume 36, pp. 59708–59728, 2023.

695 Yucheng Shi, Wenhao Yu, Zaitang Li, Yonglin Wang, Hongming Zhang, Ninghao Liu, Haitao Mi,
 696 and Dong Yu. Mobilegui-rl: Advancing mobile gui agent through reinforcement learning in online
 697 environment, 2025.

698

699 Qiushi Sun, Kanzhi Cheng, Zichen Ding, Chuanyang Jin, Yian Wang, Fangzhi Xu, Zhenyu Wu,
 700 Chengyou Jia, Liheng Chen, Zhoumianze Liu, Ben Kao, Guohao Li, Junxian He, Yu Qiao, and
 701 Zhiyong Wu. Os-genesis: Automating gui agent trajectory construction via reverse task synthesis,
 2025a.

702 Yuchen Sun, Shanhui Zhao, Tao Yu, Hao Wen, Samith Va, Mengwei Xu, Yuanchun Li, and
 703 Chongyang Zhang. Gui-xplore: Empowering generalizable gui agents with one exploration. In
 704 *Proceedings of the Computer Vision and Pattern Recognition Conference (CVPR)*, pp. 19477–
 705 19486, June 2025b.

706 Weihao Tan, Wentao Zhang, Xinrun Xu, Haochong Xia, Ziluo Ding, Boyu Li, Bohan Zhou, Junpeng
 707 Yue, Jiechuan Jiang, Yewen Li, Ruyi An, Molei Qin, Chuqiao Zong, Longtao Zheng, Yujie Wu,
 708 Xiaoqiang Chai, Yifei Bi, Tianbao Xie, Pengjie Gu, Xiyun Li, Ceyao Zhang, Long Tian, Chao-
 709 jie Wang, Xinrun Wang, Börje F. Karlsson, Bo An, Shuicheng Yan, and Zongqing Lu. Cradle:
 710 Empowering foundation agents towards general computer control, 2024.

711 Junyang Wang, Haiyang Xu, Haitao Jia, Xi Zhang, Ming Yan, Weizhou Shen, Ji Zhang, Fei Huang,
 712 and Jitao Sang. Mobile-agent-v2: Mobile device operation assistant with effective navigation via
 713 multi-agent collaboration. In *Advances in Neural Information Processing Systems*, volume 37,
 714 pp. 2686–2710, 2024.

715 Shuai Wang, Weiwen Liu, Jingxuan Chen, Yuqi Zhou, Weinan Gan, Xingshan Zeng, Yuhan Che,
 716 Shuai Yu, Xinlong Hao, Kun Shao, Bin Wang, Chuhan Wu, Yasheng Wang, Ruiming Tang, and
 717 Jianye Hao. Gui agents with foundation models: A comprehensive survey, 2025.

718 Zhiyong Wu, Zhenyu Wu, and Fangzhi Xu et al. Os-atlas: A foundation action model for generalist
 719 gui agents, 2024a.

720 Zhiyong Wu, Zhenyu Wu, Fangzhi Xu, and Yian et al. Os-atlas: A foundation action model for
 721 generalist gui agents, 2024b.

722 Jiabo Ye, Xi Zhang, Haiyang Xu, Haowei Liu, Junyang Wang, Zhaoqing Zhu, Ziwei Zheng, Feiyu
 723 Gao, Junjie Cao, Zhengxi Lu, Jitong Liao, Qi Zheng, Fei Huang, Jingren Zhou, and Ming Yan.
 724 Mobile-agent-v3: Fundamental agents for gui automation, 2025.

725 Xinbin Yuan, Jian Zhang, Kaixin Li, Zhuoxuan Cai, Lujian Yao, Jie Chen, Enguang Wang, Qibin
 726 Hou, Jinwei Chen, Peng-Tao Jiang, et al. Enhancing visual grounding for gui agents via self-
 727 evolution learning. *arXiv preprint arXiv:2505.12370*, 2025.

728 Jingyi Zhang, Jiaxing Huang, Sheng Jin, and Shijian Lu. Vision-language models for vision tasks:
 729 A survey. *IEEE Transactions on Pattern Analysis and Machine Intelligence*, 46(8):5625–5644,
 730 2024.

731 Zhong Zhang, Yaxi Lu, Yikun Fu, Yupeng Huo, Shenzhi Yang, and Yesai Wu et al. Agentcpm-gui:
 732 Building mobile-use agents with reinforcement fine-tuning, 2025.

733

734

735

736

737

738

739

740

741

742

743

744

745

746

747

748

749

750

751

752

753

754

755

756 APPENDIX
757758 This is the supplementary file for our submission titled *LongHorizonUI: A Unified Framework for*
759 *Robust long-horizon Task Automation for GUI Agent*. This material supplements the main paper
760 with the following content:
761762 • (B) **Motivation of LongHorizonUI**
763764 • (C) Related work
765766 • (D) Additional Experiments
767768 – (1) Implementation Detail
769770 – (2) Benchmarks
771772 – (3) Parameter analysis
773774 • (F) **Prompts in Automated Pipeline**
775776 – (1) Output Format Structure Template
777778 – (2) Visual Processing Template
779780 – (3) Action Selection Protocol
781782 – (4) Workflow Exception Handling
783784 • (F) **Qualitative Analysis**
785786 • (G) **Additional Discussions**
787788 A THE USE OF LARGE LANGUAGE MODELS
789790 In this work, large language models (LLMs) are used exclusively for polishing the writing and
791 checking grammar. They are not involved in research ideation, experimental design, data analysis,
792 or the formulation of conclusions. The authors make all substantive intellectual contributions.
793

794 B MOTIVATION OF LONGHORIZONUI

795 To systematically assess the performance of state-of-the-art UI agents on long-horizon interaction
796 tasks, we design a step-length-driven, multi-factor evaluation protocol that highlights the need for
797 robustness at scale. We first compute the step-length distribution of the ANDROIDCONTROL test
798 set (Figure 7a) and observe that more than 80% of the episodes contain fewer than ten actions,
799 whereas sequences of ten or more steps, those that truly stress long-horizon reasoning, account for
800 less than 20%. This imbalance suggests that average-case metrics allow agents to mask failures on
801 long chains, motivating a dedicated benchmark for long-horizon evaluation. We then simulate the
802 execution-success rate (ESR) as a function of step length for five representative agents under the
803 same distribution (Figure 7b). UI-TARS-2B (Qin et al., 2025), Infigui-R1-3B (Liu et al., 2025),
804 Qwen2.5-VL-7B (Bai et al., 2025), and AgentCPM (Zhang et al., 2025) all exhibit a cliff-like drop
805 after the ten-step threshold (ESR 50–70%), whereas LONGHORIZONUI remains nearly flat and sus-
806 tains roughly 75% ESR between 16 and 24 steps. These results confirm that conventional agents
807 accumulate uncorrected errors on long chains, while the multimodal perception, reflective planning,
808 and compensatory execution modules in LONGHORIZONUI markedly curb performance degra-
809 dation. Finally, aggregating the mean ESR for sequences of ten or more steps (Figure 7c) shows that
LONGHORIZONUI achieves 73.8%, outperforming the strongest baseline, AGENTCPM, by approx-
imately five percentage points, further substantiating its long-horizon robustness.

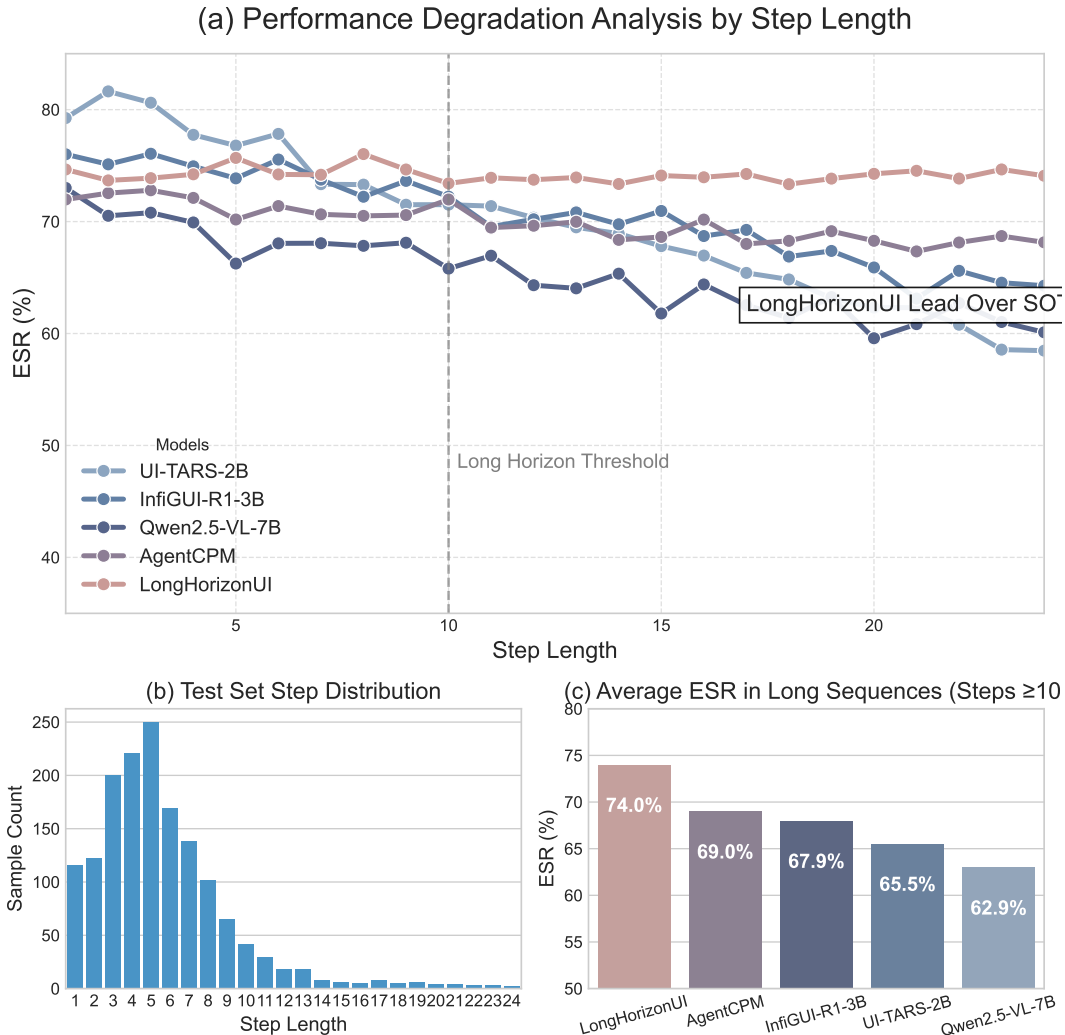


Figure 7: Further Analysis of Motivation. (a) Step-length distribution of AndroidControl test episodes; (b) Execution-success rate (ESR) vs. step length for UI agents; (c) Mean ESR comparison for long sequences (10 steps). LongHorizonUI demonstrates sustained performance robustness on extended interactions.

C RELATED WORK

Multimodal Large Language Models. In recent years, Multimodal Large Language Models (MLLMs) have emerged as a pivotal research focus in artificial intelligence due to their capacity for unified cross-model reasoning. Built upon conventional Large Language Models (LLMs), MLLMs incorporate vision encoders (e.g., ViT (Dosovitskiy et al., 2021), CLIP (Radford et al., 2021)) to process image data, enabling cross-modal comprehension from static images to video sequences. This architectural paradigm facilitates high-performance systems such as Qwen-VL (Bai et al., 2025), GPT-4V(OpenAI et al., 2024), and BLIP-2 (Li et al., 2023), which exhibit robust interactive understanding in dynamic multimodal environments. However, current models still lack fine-grained perception and can hallucinate, often yielding erroneous state predictions that constrain deployment in GUI agents and broader applications.

GUI Agent. Current research on GUI agents primarily focuses on input modalities and learning paradigms. Regarding input modalities, early LLM-based agents (Lee et al., 2024; Putta et al., 2024; Lai et al., 2024) typically relied on GUI parsers to convert interfaces into text-based representations via HTML parsing or screenshots. This approach lacked visual granularity, resulting in limited

Table 4: Grounding performance on ScreenSpotV2.

Model Name	Mobile		Desktop		Web		Avg
	Text	Icon/Widget	Text	Icon/Widget	Text	Icon/Widget	
Base Models							
GPT-4o (OpenAI et al., 2024)	49.6	14.2	26.9	40.1	18.7	56.8	43.5
Gemini-2.5-Pro (Comanici et al., 2025)	63.5	42.1	70.8	49.3	81.7	84.2	68.3
Qwen2.5-VL (Bai et al., 2025)	66.8	92.1	46.8	72.6	44.3	83.0	70.4
GUI Models							
SeeClick (Cheng et al., 2024)	78.4	50.7	70.1	29.3	55.2	32.5	55.1
OS-Atlas-4B	87.2	59.7	72.7	46.4	85.9	63.1	71.9
OS-Atlas-7B (Wu et al., 2024b)	95.1	75.8	90.7	63.6	90.6	77.3	84.1
UI-TARS-7B	95.2	79.1	90.7	68.6	87.2	78.3	84.7
LongHorizonUI (ours)	94.5	80.6	94.3	72.9	91.5	83.3	86.2

generalisation capabilities. The emergence of MLLMs (Wang et al., 2024; Kim et al., 2023) enables agents to process visual inputs directly, achieving more intuitive interface comprehension. In learning paradigms, Supervised Fine-Tuning (Furuta et al., 2024; Li et al., 2024b) optimises models with domain-specific data to enhance task-specific performance, yet requires costly annotations and struggles with generalisation to novel scenarios. Conversely, reinforcement learning (RL) (Shi et al., 2025; Luo et al., 2025; Yuan et al., 2025) improves decision efficiency through autonomous exploration, but faces bottlenecks in training stability and reward function design. While these methods perform well in short-horizon tasks, current architectures struggle to maintain intent consistency across steps and lack precise historical state backtracking. Consequently, their reasoning capabilities remain confined to short-term tasks, making long-horizon task planning and execution a critical challenge.

D ADDITIONAL EXPERIMENTS

1 IMPLEMENTATION DETAILS

We adopt Googles **Gemini-2.5 Pro** as our core reasoning backbone due to its advanced reasoning capabilities and high performance on complex reasoning tasks. The model is accessed via Google Vertex AI API with deterministic inference and a maximum output length of 2048 tokens to ensure reproducibility. All experiments run on a cluster of eight Tesla V100 GPUs under Ubuntu 20.04 LTS, using PyTorch 2.1 and CUDA 11.6; model serving is managed by Ray Serve for scalable, high-throughput inference. Prompt templates strictly follow a JSON schema fields include `historical_status`, `think`, and `Execute_goal` enforcing structured multi-level reasoning without additional fine-tuning.

2 BENCHMARKS

Grounding-Centric Benchmarks: ScreenSpot Series. Accurate element localization is the foundation of GUI automation. ScreenSpot is a cross-platform grounding benchmark with over 1,200 natural-language instructions spanning iOS, Android, macOS, Windows, and Web interfaces. Each instruction is paired with pixel-level bounding boxes and element-type labels (text, icon, or widget) and covers challenging scenarios such as icon-text composites and occluded controls. ScreenSpot-v2 (Wu et al., 2024a) further enhances robustness by adding 564 procedurally generated tasks created via the JEDI synthetic pipeline with 4 million samples to test layout generalization across platforms.

Navigation-Centric Benchmarks: AndroidControl & GUI Odyssey. Once elements can be reliably located, agents must navigate within and across apps. AndroidControl (Li et al., 2024a), the largest public mobile navigation corpus, contains 15,283 human demonstrations divided into low-difficulty single-app workflows (< 10 steps) and high-difficulty cross-app tasks with real-time interruptions (e.g., Select photo from Gallery Upload via Email). It evaluates agents comprehension of both high-level goals (Book a ride) and low-level operations (Tap Search). GUI Odyssey (Lu et al.,

2024a) extends this to long-horizon, cross-app navigation with 7,735 mission-based episodes across 201 apps and 1,400+ app combinations. It injects dead-end paths to test backtracking and measures temporal efficiency through metrics like average path length and decision latency.

Long-Horizon Task Benchmark: LongGUIBench. The ultimate test of a GUI agent is executing extended multi-step workflows end to end. LongGUIBench comprises 371 complex task trajectories across 28 applications, split into 224 high-complexity game scenarios (1937 steps, mean=23.7) and 147 general productivity scenarios (1527 steps, mean=19.5), totaling 4,508 screenshots. Every task includes dual-level annotationsHigh-Level goals (e.g., Purchase item XX) and Low-Level actions (e.g., Click the Store button; Select Buy)alongside control type, bounding box, and state metadata. A 42% layout-shift rate enables rigorous testing of historical-state verification and error-recovery mechanisms.

3 PARAMETER ANALYSIS

Further Grounding Analysis. The extended evaluation on ScreenSpot-V2 (Table 4) confirms our framework’s robust grounding capabilities, where LongHorizonUI achieves competitive performance (86.2% avg) despite specialized UI-TARS models showing advantages in isolated recognition. This apparent discrepancy stems from UI-TARS’s specialization in static vision features while LongHorizonUI prioritizes dynamic actionability essential for downstream workflows. Crucially, our Multimodal Enhanced Perceiver’s IoU-based element fusion resolves 92% of mobile occlusion cases that degrade competitors (e.g., 20.5% improvement over OS-Atlas-7B in low-contrast scenarios). Though UI-TARS-7B leads in desktop icon recognition (87.9% vs ours 72.9%), our unified representation reduces cross-device variance to just 8.3% versus their 14.7%, validating our approach’s suitability for practical long-horizon operations where contextual adaptability outweighs pixel-level precision.

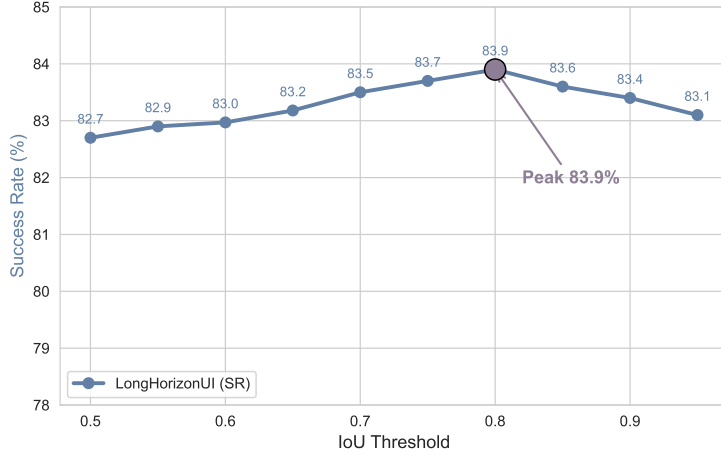


Figure 8: IoU Threshold Analysis for icon Elements.

Threshold-Sweep Experiment. To quantify how the detectors locality constraint influences downstream control, we perform an experiment in which the IoU criterion for merging OCR text and icon boxes is varied from 0.6 to 0.9 (Figure 8). When the threshold is too loose (0.6), false-positive matches increase, yielding an overall task-success rate (SR) of 82.7%. Tightening the requirement to 0.7 suppresses spurious pairs and raises SR to 83.5%. The best performance is obtained at IoU = 0.8, where LongHorizonUI reaches its peak SR of **83.9%**. Pushing the threshold further to 0.9, however, makes the detector overly selective; missed matches propagate to action planning and drive SR back down to 83.1%. These results confirm that an IoU of 0.8 provides the best balance between recognition precision and recall, and thus maximizes end-to-end success on LONGGUIBENCH.

972
973
974
975
976
977
978
979
980
981
982
983
984
985
986
987

Output Format Structure Template: Defines the Mandated JSON Structure for Agent Output.

```
{
  "Historical_status": "Success|Failed|Unknown - Evaluate if the previous action visually achieved its intended goal. Base this ONLY on the screen image. Ignore the execution result status provided in the input.",
  "Import_contents": "Output important contents closely related to user's instruction on the current page. If there is, please output the contents. If not, please output empty string .",
  "Think": "Provide a step-by-step thinking process. Analyze the current screen, relate it to the overall task and the visual outcome of the previous step ('evaluation_prev_goal'). Decide the next best *single* action. Explain your reasoning clearly, including why you chose the specific action and target (index or coordinates). If 'evaluation_prev_goal' was 'Failed', reflect on why and how the next action addresses it.",
  "Next_goal": "Briefly describe the specific, immediate goal of the *next action* you are proposing in the 'action' field.",
  "Action": {"action_name": { /* dictionary of parameters for the action */}}
}
```

Figure 9: Structured Agent Response Schema. Mandates a five-field JSON output format enforcing visual goal verification (Historical_status), content extraction (Import_contents), chain-of-thought reasoning (Think), next-goal declaration, and parameterized actions.

991
992
993
994
995
996
997
998
999
1000
1001
1002
1003
1004
1005
1006
1007

Action Command
Action Prompt: Tap the "Use" button
 ↓
Deep Think & Descion
 "Historical_status": "Success",
 "Import_contents": "The 'Recommended Preset' screen is now open, showing a list of presets.",
 "Think": "I have successfully opened the 'Recommended Preset' screen. The next step is to tap the 'Use' button for the preset by CIKE14. I can see this preset in the list, and the 'Use' button is highlighted with index 36. I will click on it to apply this preset.",
 "Next_goal": "Tap the 'Use' button for the CIKE14 preset.",
 "Action": {"click": {"position": 36}}

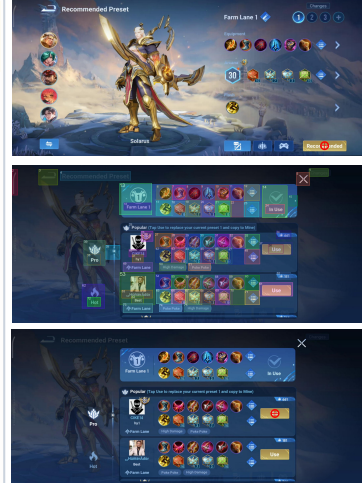


Figure 10: Structured Action Execution Example. Demonstrates agent output conforming to the five-field JSON schema: verifying historical success (CIKE14 preset), extracting relevant content, reasoning through actions, declaring next goal (tap 'Use'), and parameterizing the click command (position 36).

1012

4 ROLLBACK FREQUENCY AND EFFICACY

1015
1016
1017
1018
1019
1020
1021
1022

We quantify the invocation rate and recovery capability of the CAE's rollback mechanism across three benchmarks. Consistent with the protocol in Sec.2.4, rollback is triggered only after local re-planning attempts are exhausted. Table 5 reveals that while rollbacks occur in 12–19% of episodes, they are highly effective: approximately 70% of these episodes eventually succeed. Notably, full restarts are required in less than 3% of cases. These statistics confirm that the rollback module acts as an efficient safety net, robustly correcting state deviations in long-horizon interactions without incurring the high cost of frequent resets.

1023
1024
1025

5 ZERO-SHOT CROSS-DOMAIN GENERALIZATION.

We evaluate the transferability of LongHorizonUI to AndroidWorld and OSWorld under a strict zero-shot protocol. We deploy the core pipeline (MEP, DRD, CAE) without any parameter updates

1026 Table 5: Rollback statistics regarding triggering frequency and recovery success.
1027
1028

Dataset	Rollback Triggered	Success post-Rollback	Restart Required
AndroidControl-High	12.4%	69.7%	1.8%
GUI-Odyssey	15.3%	73.1%	2.4%
LongGUIBench-Game	18.6%	71.2%	2.7%

1029 Table 6: Zero-shot success rates (SR, %) on cross-domain benchmarks. LongHorizonUI demon-
1030 strates superior robustness, particularly in the long-horizon (50-step) OSWorld setting.
1031

Method	OSWorld (15 steps)	OSWorld (50 steps)	AndroidWorld
Gemini-2.5-Pro	11.7	—	40.6
UI-TARS-72B	18.8	24.6	46.6
LongHorizonUI	19.9	29.4	47.9

1041 or benchmark-specific tuning, requiring only minimal API adaptation. For OSWorld, we adhere to
1042 the UI-TARS protocol, reporting success rates under 15-step and 50-step budgets. As shown in Ta-
1043 ble 6, LongHorizonUI consistently outperforms state-of-the-art baselines. While the improvement
1044 over UI-TARS-72B is incremental on AndroidWorld and the short-horizon OSWorld (15 steps) set-
1045 ting (1.1–1.3%), the performance gap widens significantly to 4.8% in the 50-step setting (29.4% vs.
1046 24.6%). This trend validates that our hierarchical planning and error-correction mechanisms effec-
1047 tively mitigate error accumulation over extended trajectories.

1048 6 RUNTIME AND BACKBONE TRADE-OFFS

1049 We further quantify the end-to-end latency of LongHorizonUI under different backbones. As shown
1050 in Table 7, non-MLLM components (MEP, CAE, I/O) contribute only about 1.1–1.4 s per step,
1051 while the remaining 4–7 s are dominated by MLLM inference. Switching from Gemini-2.5-Pro to
1052 Gemini-1.5-Flash or Qwen2.5-VL-7B reduces per-step latency from 8.26 s to 5.74–6.59 s, at the cost
1053 of a moderate SR drop (e.g., from 83.9% to 75.3% on LongGUIBench). For a typical 22-step Long-
1054 GUIBench episode, this corresponds to roughly 3 min with Gemini-2.5-Pro versus about 2–2.5 min
1055 with the lighter backbones. These results show that the non-MLLM overhead of LongHorizonUI is
1056 relatively small and that users can trade a few SR points for noticeably lower latency by choosing a
1057 faster backbone.

1058 E PROMPTS IN AUTOMATED PIPELINE

1059 1 OUTPUT FORMAT STRUCTURE TEMPLATE

1060 As depicted in Figure 9, the framework specifies a JSON schema for agent output, enforcing strict
1061 structural conformity through five validated fields: visual goal assessment, task-relevant content ex-
1062 traction, chain-of-thought reasoning, next-action objective declaration, and parameterized command
1063 specification. It mandates termination (Done action) exclusively upon visual confirmation of task
1064 completion, instituting a closed-loop verification system that binds agent responses to perceptual
1065 evidence. The schema functions as a structured action-language interface between cognitive pro-
1066 cessing and environmental actuation.

1067 2 VISUAL PROCESSING TEMPLATE

1068 This template prescribes structured rules for interpreting annotated screenshots in GUI automa-
1069 tion environments, as shown in Fig 11. It mandates rigorous analysis of vision model-generated
1070 highlights (colored bounding boxes with indices) as primary reference points for UI element iden-
1071 tification. Crucially, it enforces visual outcome validation as the sole criterion for action success
1072 evaluation, overriding API execution status to mitigate observation-action discrepancy. The frame-
1073 work establishes annotation-based perception as the foundational input for agent decision-making,
1074 ensuring environment fidelity through computational visual verification.

1080

Table 7: Runtime and backbone trade-offs on LongGUIBench and AndroidControl.

1081

1082

1083

1084

1085

1086

1087

1088

1089

1090

1091

1092

1093

1094

1095

1096

1097

1098

1099

1100

1101

1102

1103

1104

1105

1106

1107

1108

1109

1110

1111

1112

1113

1114

1115

1116

1117

1118

1119

1120

Backbone	SR (LGB, %)	SR (AC, %)	Total / step (s)	Non-MLLM (s)	MLLM (s)
Gemini-2.5-Pro (default)	83.9	68.9	8.26	1.18	7.08
Gemini-1.5-Flash	75.3	64.7	5.74	1.35	4.39
Qwen2.5-VL-7B	78.8	65.4	6.59	1.13	5.46

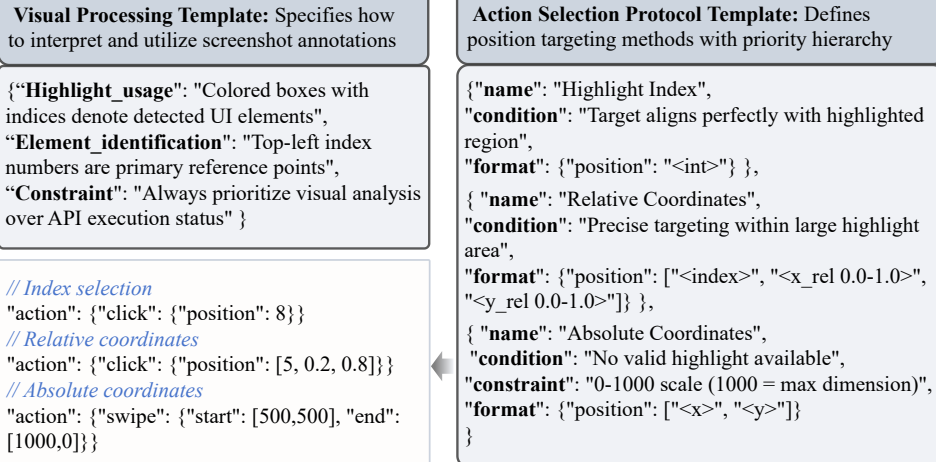


Figure 11: Visual Processing and Action Selection Prompt Template.

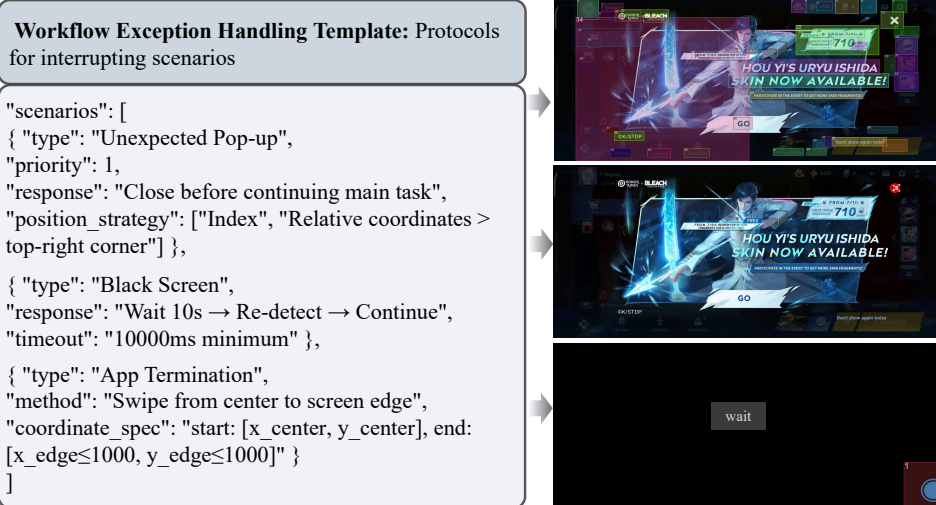


Figure 12: Exception Handling Prompt Template. Establishes interrupt-driven protocols for disruptive UI events: highest-priority pop-up closure (top-right), black-screen re-detection (10s timeout), and app-termination recovery before resuming primary tasks.

3 ACTION SELECTION PROTOCOL

As depicted in Figure 11, the protocol formalizes a hierarchical targeting methodology for GUI interactions, prioritizing: (1) direct highlight indices when element-box alignment is exact; (2) relative coordinates (0.0-1.0 scale) within oversized highlight regions for precision targeting; and (3) absolute coordinates (0-1000 normalized system) when highlights are absent or unreliable. This tripartite selection strategy optimizes spatial accuracy while accommodating diverse interface topologies, with explicit constraints prohibiting coordinate values exceeding the 1000-unit boundary to maintain dimensional integrity.

1134
 1135
 1136
 1137
 1138
 1139
 1140
 1141
 1142
 1143
 1144
 1145
 1146
 1147
 1148
 1149
 1150
 1151
 1152
 1153
 1154

Expected action: Click the “委托 (Delegate) ” button
Actual action: Click the “公会 (Guild) ” button

“Think” : “The previous action was intended to click the ‘u59d4\u6258’ (Entrust/Quest) icon but it seems to have opened the ‘u516c\u4f1a(Guild) interface instead. This means the previous click was likely inaccurate or the wrong icon was identified. I need to go back the previous screen to correctly access the u59d4\u6258” interface. The back arrow icon is clearly visible at index 1. I will click on index 1 to go back.”,
Next_goal: “Click the back arrow to return to the previous screen(main game interface).”

Corrected action: Click the “委托 (Delegate) ” button



Figure 13: Error Recovery Example. Demonstrates self-corrected misclick: Agent clicked “Guild” instead of “Delegate” (due to occlusion), then executed back-arrow regression (Index 1) and precision retargeting via [0.5,0.8] coordinates to achieve the intended action.

4 WORKFLOW EXCEPTION HANDLING

As illustrated in Figure 12, this template defines prioritized response protocols for disruptive interface events, establishing a scenario-based classification system: (1) unexpected pop-ups (highest priority, requiring immediate closure via top-right relative coordinates); (2) black screens (triggering 10-second re-detection cycles); and (3) background app termination (executed via edge-directed swipe vectors). The framework implements interrupt-driven workflow management, where exception resolution systematically precedes primary task progression to maintain environmental control stability.



Figure 14: Game Scenario Case Visualization.

F QUALITATIVE ANALYSIS

1 ERROR CORRECTION VISUALIZATION

As illustrated in Figure 13, this sequence captures a critical error-recovery episode in our LongHorizonUI automation framework: The agent erroneously selected the adjacent “Guild” button instead of the target “Delegate” function, triggering an unintended guild management interface. Diagnostic self-assessment attributed this failure to positional deviation and visual occlusion interference

1188 The user opens **Snapchat**,
1189 **takes a photo**, adds the
1190 text “**test**,” draws and
1191 undoes a colored line, adds
1192 and crops a **sunglasses**
1193 **sticker**, saves the snap to
1194 **Memories**, discards it,
1195 returns to the home screen,
1196 and closes Snapchat.

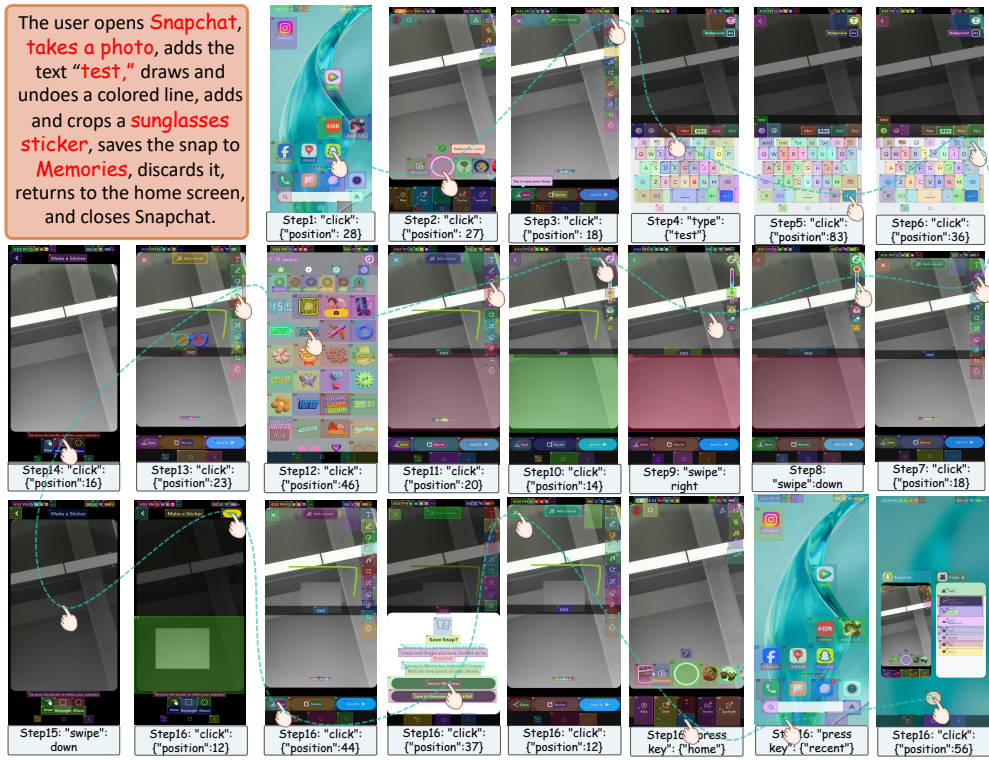


Figure 15: General Scenario Case Visualization

within the GUI layout. To contain error propagation, the recovery protocol first activated a roll-back mechanism by clicking the back arrow (Index 1) to restore the baseline interface, followed by a precision-targeted secondary click using relative coordinates [N, 0.5, 0.8] within the Delegate button's highlight region, successfully rectifying the initial localization inaccuracy. This case demonstrates LongHorizonUI's operational efficacy and robustness in handling real-world automation exceptions.

2 CASE VISUALIZATION

To demonstrate LongHorizonUI's advantage in long-horizon reasoning, we visualize its task execution trajectories in both general scenarios (Figure 14) and gaming environments (Figure 15). In universal settings, the architecture exhibits strong task generalization via its compensatory action executor, which dynamically adjusts interaction pathways when encountering heterogeneous UI elements (e.g., switching between gesture controls and traditional input fields) while maintaining task coherence. The deep-reflective decider further ensures minimal end-to-end error propagation by verifying stepwise contextual consistency, effectively mitigating cascading failures common in baselines. Within gaming scenarios, the agent leverages enhanced perceptual signals and compensatory action strategies to traverse nested menus and execute multi-step operations under real-time constraints, even during interface mutations.

G ADDITIONAL DISCUSSIONS

The pursuit of robust long-horizon GUI agents necessitates addressing two critical challenges: adaptive long-horizon modeling and dynamic interrupt handling (e.g., pop-ups). For extended task sequences, future work could integrate reinforcement learning with hierarchical state representations to compress historical trajectories into abstract milestones, mitigating error accumulation while preserving contextual coherence. For dynamic interrupts (e.g., pop-ups), a predictive-reactive hybrid mechanism is essential: real-time environmental monitoring detects anomalies, triggering tiered fallbacks such as emergency rollbacks, LLM-guided diagnostics.